

CALPHAD MODELLING OF CERAMIC SYSTEMS

K. C. Hari Kumar¹, Soumya Sridar¹¹Department of Metallurgical and Materials Engineering, Indian Institute of Technology Madras,
Chennai 600 036, INDIA

Abstract: Thermodynamic modeling based on the CALPHAD approach is a powerful tool for understanding the behavior and designing materials with optimized properties. This method relies on the availability of relevant Gibbs energy functions. The present work is concerned with developing the Gibbs energy functions for Si-Zr-N and Ti-Zr-N systems. The outcome of implementing such an approach is a set of internally consistent Gibbs energy functions for various phases. These functions are used to build Gibbs energy databases for multicomponent systems that are accessed by Gibbs energy minimization software to compute phase diagrams and thermochemical properties. They can be used to compute the thermochemical and constitutional information that would help in understanding the behavior of these materials and optimizing their compositions for different applications.

1. Introduction

The development of superhard materials for extreme environment applications is a subject of great importance. Most of the cutting tools and other components, subjected to friction and wear are coated with superhard materials. Though the durability of these coatings depends on mechanical properties such as hardness and wear resistance, their high-temperature oxidation resistance is also important. The excessive oxidation of these coatings leads to loss of adherence and reduction in wear resistance.

TiN and ZrN are used as protective coatings for cutting and forming tools due to their high hardness and wear resistance. Though these coatings possess excellent mechanical properties, their oxidation resistance at elevated temperatures is poor. It was reported that the oxidation resistance of these coatings can be enhanced by the incorporation of silicon [1]. The highest oxidation resistance was achieved in Si-Zr-N coatings containing about 10 mol% Si as reported by [2]. Cemented carbide tips coated with the mixed nitride (Ti, Zr)N have shown improved cutting performance due to the alloying effect of Zr with Ti in the fcc-TiN unit cell [3]. At high cutting speeds, spinodal decomposition can be expected to occur because of an increase in temperature at the contact zone, leading to a further increase in hardness and wear resistance [4].

The main aim of this work is to explore the phase equilibria and thermochemistry of ternary nitride coatings for tribological applications using the CALPHAD method. It is possible to obtain the thermochemical and constitutional information with the help of Gibbs energy functions for individual phases using this method. This information will be beneficial for the selection, processing, and application of these materials for various applications. In this study, an internally consistent set of Gibbs energy functions for various phases are obtained using the CALPHAD approach combined with ab initio calculations for Si-Zr-N and Ti-Zr-N systems.

These functions are an integral part of Gibbs energy databases for multicomponent systems that are accessible to Gibbs energy minimization software such as Thermo-Calc [5].

2. The Calphad method

The term CALPHAD is the acronym for CALculation of PHase Diagrams. This method combines the classical thermodynamic principles with mathematical formulations that facilitate the calculation of thermochemical properties and phase equilibria of multicomponent multiphase systems. The CALPHAD approach is based on the principle that state variables corresponding to thermodynamic equilibrium can be computed using Gibbs energy minimization. The required functions for multicomponent systems can be obtained by combining the Gibbs energy functions of

the bounding binary systems. Correction terms are usually required to account for the higher-order effects, usually not exceeding the ternary effects. Hence, the central theme of this approach is Gibbs energy modeling. The main task of this approach is, thus, to develop a consistent set of Gibbs energy functions for relevant phases in the bounding binary and ternary systems that reproduce the experimental information satisfactorily. The foundation for this method was laid by van Laar [6], who calculated binary phase diagrams using ideal and regular solution models. In 1970, Kaufman and Bernstein [7] introduced the idea of lattice stability. This concept along with the Gibbs energy models for developing phase diagrams from experimental data led to the computer calculation of phase diagrams.

2.1. Gibbs energy models

2.1.1 Elements

Elements and stoichiometric compounds have fixed composition and hence, their Gibbs energies will be dependent only on pressure and temperature. The Gibbs energy of an element in a chosen structural state can be expressed as the following.

$$G(T, p) = G^{\text{ch}} + G^{\text{ph}} + G^{\text{pr}} \quad (1)$$

where G^{ch} is the chemical (lattice) contribution, G^{ph} is the physical contribution, typically due to magnetic ordering and G^{pr} is the pressure contribution. The functions recommended by Scientific Group Thermodata Europe (SGTE) [8] are to be used for G^{ch} , which has the following format (Meyer-Kelly polynomial).

$$G_i^\circ(T) = H_i^{\text{SER}} + a + bT + cT \ln T + dT^2 + eT^{-1} + fT^3 + \dots \quad (2)$$

where, a, b, c, . . . are the model parameters. $^\circ$ indicates that standard pressure (1 bar) is used. SER refers to the Stable Element Reference i.e., with respect to the enthalpy at 298.15 K and 1 bar (H_i^{SER}) and entropy at 0 K, which is zero according to the third law of thermodynamics. Similarly, the Gibbs energy as a function of temperature for a stoichiometric compound θ is as follows.

$$G^{\circ, \theta}(T) = \sum_i \nu_i H_i^{\text{SER}} + A + BT + CT \ln T + DT^2 + ET^{-1} + FT^3 \dots \quad (3)$$

where, A, B, C, . . . are the model parameters. ν_i are the stoichiometric coefficients of the elements that make up θ . These functions are generally valid above room temperature.

2.1.2 Solutions

The general form of Gibbs energy of a solution is

$$G = G^{\text{ref}} + G^{\text{conf}} + G^{\text{E}} + G^{\text{ph}} + G^{\text{pr}} \quad (4)$$

where G^{ref} is the reference term and can be considered as Gibbs energy of a mechanical mixture of the constituents. G^{conf} refers to the contribution from ideal mixing of constituents and G^{E} is the excess contribution that accounts for deviation from ideal behavior. The exact form of these terms depends on the Gibbs energy model chosen for a phase.

Random substitutional solutions

A substitutional solution model is one of the simplest mixing models, where the solute atoms substitute the solvent atoms randomly. For a multicomponent random substitutional solution at

standard pressure, the G^{ref} in Equation 4 can be written as

$$G^{ref} = \sum_i x_i (G_i^{\circ} - H_i^{SER}) \quad (5)$$

where, x_i is the mole fraction of component i . The G^{conf} can be represented as

$$G^{conf} = RT \sum_i x_i \ln x_i \quad (6)$$

The composition dependence of G^E term in Equation 4 can be expressed by Redlich-Kister (R-K) polynomial [9]. Using this polynomial, the G^E for the random-substitutional solution in a system A-B can be written as

$$G^E = x_A x_B \sum_{\nu=0}^n {}^{\nu}L_{A,B} (x_A - x_B)^{\nu} \quad (7)$$

where, ${}^{\nu}L_{A,B}$ is the R-K polynomial coefficient of ν^{th} order. The temperature dependence of these parameters can be represented as

$${}^{\nu}L_{A,B} = {}^{\nu}a + {}^{\nu}bT + {}^{\nu}cT \ln T \quad (8)$$

In the case of multicomponent solutions, the excess Gibbs energy (G_{m-c}^E) can be written in terms of the excess Gibbs energies of the constituent binaries (G_{i-j}^E) using geometrical extrapolation. Although there are many geometrical extrapolation schemes available, the Muggianu extrapolation [10] along with R-K polynomials is preferred due to its simplicity. Hence, for a multicomponent solution with random mixing, the excess Gibbs energy can be represented as

$$G_{m-c}^E = \sum_{i=1}^{c-1} \sum_{j=i+1}^c G_{i-j}^E(x_i, x_j) + \text{correction terms} \quad (9)$$

where, c is the number of components. The correction terms represent the contributions from the higher-order systems, generally not exceeding ternary or quaternary systems. The excess Gibbs energy for a ternary random substitutional solution (G_{1-2-3}^E) can be represented as

$$G_{1-2-3}^E = \sum_{i=1}^2 \sum_{j=i+1}^3 G_{i-j}^E(x_i, x_j) + x_1 x_2 x_3 L_{1,2,3} \quad (10)$$

where, $L_{1,2,3}$ is the ternary correction term.

Sublattice formalism

A simple mixing model such as the random-substitutional solution is not usually adequate since many phases have more than one type of site in which mixing takes place. This leads to a general modeling concept known as sublattice formalism. The concept of subdividing configuration space into sublattices was introduced by [11] to describe the thermodynamics of reciprocal salt systems. In this model, it was proposed that the anions and cations occupy separate sublattices and the mixing is random in each sublattice. This approach is very suitable for modeling a variety of phases

such as random substitutional as well as interstitial solutions, stoichiometric compounds, intermediate phases with homogeneity range, ionic melts, *etc.* This concept was adapted for other systems by [12]. It was further extended by [13] to include an arbitrary number of constituents in each sublattice. The generalized sublattice formalism with an arbitrary number of sublattices as well as constituents within each sublattice was proposed by [14]. According to this a formula unit of a phase can be represented by

$$(A, B, C \dots)_{a_1} : (A, C, E \dots)_{a_2} : \dots (B, D, E \dots)_{a_n} \quad (11)$$

where, the constituent species A, B, C... may be atoms, molecules, charged species, or vacancies (Va), and a_s is the relative number of sites in sublattice s . It is also assumed that there is random mixing among the constituents in each sublattice. Each pair of parenthesis denotes a sublattice, a colon (:) separates each sublattice and a comma (,) separates each constituent within a sublattice. It should be noted that a constituent species is allowed only once in each sublattice.

A composition variable called site fraction ($y_{i\#s}$) is introduced in order to formulate the Gibbs energy using the sublattice formalism. It is defined as the mole fraction of a constituent species i in sublattice s , i.e.,

$$y_{i\#s} = \frac{N_{i\#s}}{N_s} \quad (12)$$

where, $N_{i\#s}$ is the number of constituent species i and N_s is the total number of sites in sublattice s , including vacant sites. Using the sublattice formalism, the Gibbs energy per mole of formula unit (mfu) of a phase is given as

$$G_{\text{mfu}} = \sum_{I(0)} \left(\prod_{I(0)} y_{i\#s} \right) G_{I(0)}^\circ + RT \sum_s a_s \sum_i y_{i\#s} \ln y_{i\#s} + \sum_{I(z)} \left(\prod_{I(z)} y_{i\#s} \right) L_{I(z)} \quad (13)$$

where $I(z)$ is the constituent array of z^{th} order. An 0^{th} order constituent array ($I(0)$) has only one species occupying each sublattice. It is commonly referred to as an end-member since it resembles a stoichiometric compound. The first term in Equation 13 represents the reference term that is formed by the weighted sum of the Gibbs energies of all the end-members $I(0)$. The second term is the contribution of configurational entropy to Gibbs energy due to the random mixing of constituents within each sublattice. The excess contribution to Gibbs energy is given by the third term. It consists of several interaction energy terms $L_{I(z)}$ which arise due to the interaction of constituents within a sublattice. The interaction terms beyond the second order constituent array are not considered since their contribution to Gibbs energy is negligible. Sublattice formalism provides an appropriate method to formulate realistic mixing models for a variety of phases. Care must be taken to choose the right number of sublattices that must agree with the crystallography and homogeneity range of the phase that is considered. The use of too many sublattices is not beneficial since the Gibbs energy needs to be determined for a large number of end-members, which is not practical. Hence, for phases with complex crystal structures, one may need to simplify the model by combining sublattices based on point group symmetry, coordination number, *etc.*

Table 1: Typical settings used for VASP calculations.

Pseudopotential	PAW
Exchange-correlation functional	GGA-PBE
Energy cut-off	600 eV
k -point spacing	$\leq 0.02 \text{ \AA}^{-1}$
k -point sampling scheme	Monkhorst-Pack [17]
Force convergence	$2 \times 10^{-3} \text{ eV \AA}^{-1}$
Energy convergence	10^{-7} eV
Integration scheme	Tetrahedron method with Blöchl corrections [18]

4. Ab initio calculations

With the advancements in high-performance computing, it is now possible to carry out intensive low-length scale calculations for systems with a large number of atoms and molecules. Amongst these calculations, the total energy calculations based on density functional theory (DFT) have gained much use in the context of CALPHAD. Results from these calculations often serve as input in the thermodynamic modeling, greatly improving the quality of the Gibbs energy functions. The predictive capability of DFT can be utilized to obtain the structural, electronic, and thermodynamic properties of materials.

Thermochemical properties such as enthalpy of formation, enthalpy of mixing, *etc.* serve as important input quantities in the optimization of Gibbs energy functions. When the experimental values are unavailable, calculated values of these properties can be used in the optimization. Besides, the enthalpy of formation of hypothetical end-members of the sublattice formulation (Equation 13) may be required. These quantities can also be obtained using *ab initio* calculations based on DFT. In the past, empirical methods such as Miedema model [15] were used for estimating the enthalpy of formation. At present, methods based on DFT are being used for generating thermochemical information such as enthalpy of formation and enthalpy of mixing of a solid solution at absolute zero of temperature with good accuracy.

In the present work, DFT calculations are performed using Vienna Ab initio Simulation Package (VASP) [16]. General settings used for the calculations are listed in Table 1.

The enthalpy of formation ($\Delta_f H_{298}^\circ$) is estimated by calculating the difference between the total energies of the compound and pure elements in the chosen structural state

$$\Delta_f H_{298}^\circ \approx E_0(A_y B_z) - yE_0(A) - zE_0(B) \quad (14)$$

where, $E_0(A_y B_z)$, $E_0(A)$ and $E_0(B)$ are the total energies of compound $A_y B_z$ and elements, A and B, respectively.

The *mcsqs* [19] code of Alloy Theoretic Automated Toolkit (ATAT) [20] is used for generating the SQS supercells at different compositions. This code generates SQS structures using stochastic techniques such as the Monte Carlo method which are more efficient in finding the optimum supercell. The enthalpy of mixing, $\Delta_{\text{mix}} H$ obtained from these calculations is useful input for thermodynamic assessments. In the present work, SQS has been used to generate random mixing of the substitutional atoms in the nitrides of Ti-Zr-N and Al-B-N systems.

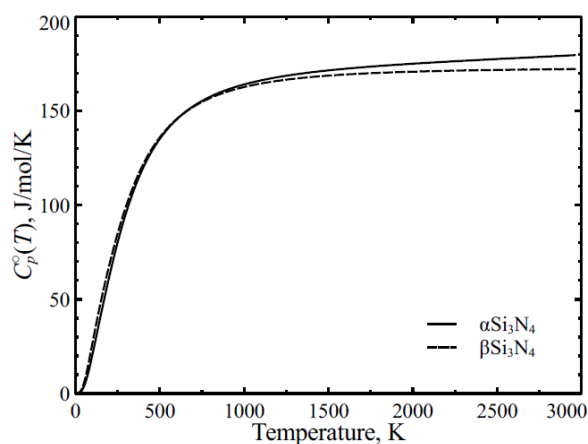


Figure 1: Calculated C_p° for α and $\beta\text{Si}_3\text{N}_4$ using QHA.

DFT calculations are capable of predicting the total energy (E_0) of a structure at 0 K. To obtain accurate Gibbs energy parameters, thermodynamic properties at finite temperature (above 0 K)

are crucial. In this work, both harmonic and quasiharmonic approximations are used for calculating the finite-temperature thermodynamic properties. The harmonic approximation is implemented using the PHONON code [21]. Phonopy [22] was used for estimating the thermodynamic properties using quasiharmonic approximation (QHA).

4. Thermodynamic optimisation

Thermodynamic optimization was performed using the PARROT module [23] of the Thermo-Calc. Details about the optimization of Si-N, Zr-N, Ti-Zr-N, and Si-Zr-N are given below.

4.1. Si-N system

Thermodynamic functions for this system are available from the work of [24]. However, it was not possible to reproduce the phase relations in Si-Zr-N system using that description. Hence, the Si-N system has been re-optimized in this work. The enthalpy of formation ($\Delta_f H_{298}^\circ$) as well as heat capacities (C_p) of and Si_3N_4 are calculated using the *ab initio* calculations mentioned above. The computed values of $\Delta_f H_{298}^\circ$ for α and $\beta\text{Si}_3\text{N}_4$ are -790012 and -788858 J/mol, respectively. The C_p as a function of temperature obtained using QHA for α and $\beta\text{Si}_3\text{N}_4$ is shown in Figure 1. The $C_p^\circ(T)$ values are fitted to appropriate expressions down to 0 K and integrated to obtain the Gibbs energy functions (Equation 15).

$${}^\circ G^{\text{Si}_3\text{N}_4} - 3H_{\text{Si}}^{\text{SER}} - 4H_{\text{N}}^{\text{SER}} = \begin{cases} a + bT + \gamma T^4 \\ a + bT + cT \ln T + dT^{-1} + eT^{-2} + fT^3 \end{cases} \quad (15)$$

The model parameters for this system are optimized using thermochemical (experimental and *ab initio*) and constitutional data as input. The calculated phase diagram is shown in Figure 2a. There is good agreement between the experimental data and the calculated phase boundaries. The phase diagram calculated without considering the gas phase is shown in Figure 2b.

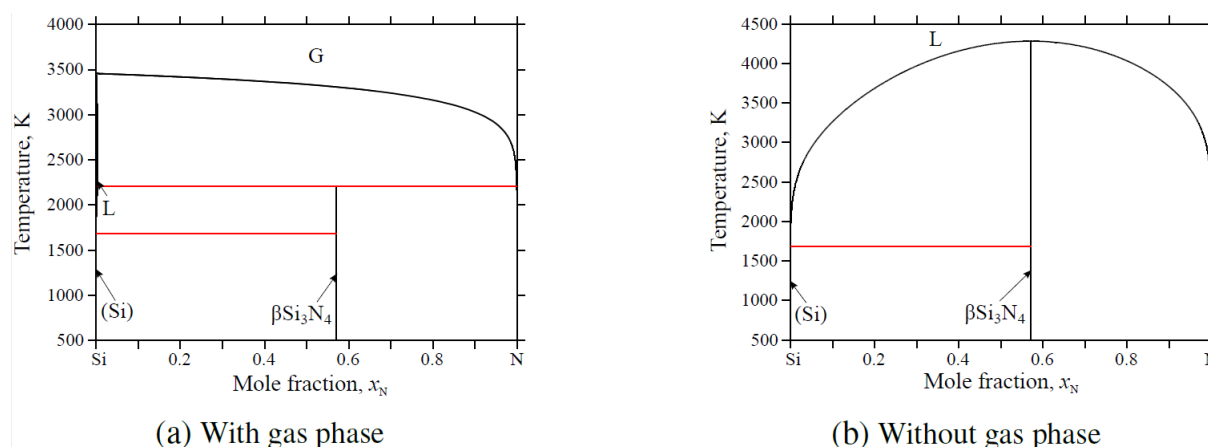


Figure 2. Calculated Si-N phase diagrams.

Table 2. Enthalpy of formation of end-members in Zr-N system using DFT

End-member	$\Delta_f H_{298}$ (J/mol)
ZrN (fcc)	-341593
ZrN _{0.5} (hcp)	-148695
ZrN ₃ (bcc)	+280996

4.2 Zr-N system

The Zr-N system was initially modeled by [25]. Since some of the critical experimental data available in the literature were not used in that work, a re-optimization of the system is done here. The computed ΔfH_{298}° values with respect to Zr(hcp) and N₂ (g) using DFT are listed in Table 2. It is to be noted that ZrN₃ and ZrN_{0.5} are the end-members of the sublattice formulations of bcc and hcp solid solutions. The Helmholtz energy estimated using harmonic approximation is converted to Gibbs energy with respect to SER using the following equation [26].

$$G_T^\circ(\text{phase}) = \sum_{i=\text{elements}} \nu_i H_{298}^\circ(i) = E_0(\text{phase}) + \text{ZPE}(\text{phase}) + A_T^\circ(\text{phase})$$

$$= \sum_{i=\text{elements}} \nu_i [E_0(i) + \text{ZPE}(i) + (H_{298}^\circ - H_0^\circ)(i) + (pV(i))] \quad (16)$$

where ZPE is the zero-point energy that was obtained from these calculations. The Gibbs energy calculated using a harmonic approximation for stoichiometric ZrN is shown in Figure 4.

This system was optimized with experimental thermochemical and constitutional data as well as the *ab initio* thermochemical data as input. The calculated Zr-N phase diagram and its comparison with experimental data show that they are in good agreement (Figure 3). The calculated Gibbs energy of ZrN matches well with the values estimated from *ab initio* calculations, as shown in Figure 4.

4.3 Ti-Zr-N system

Experimental information indicates that TiN and ZrN are immiscible with each other below 2000 K [28]. However, there is no experimental data regarding the critical point of the miscibility gap. The enthalpy of mixing of TiN and ZrN, computed using SQS, indicates that demixing is favored

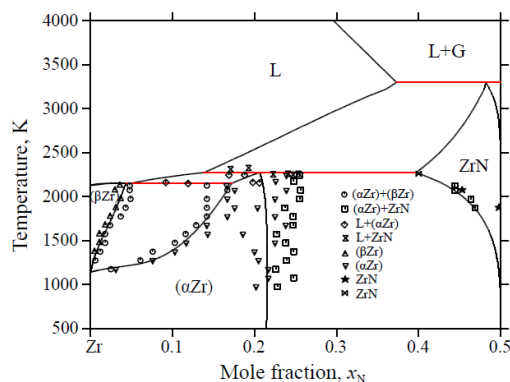


Figure 3. Comparison of calculated Zr-N phase diagram with experimental data [27]

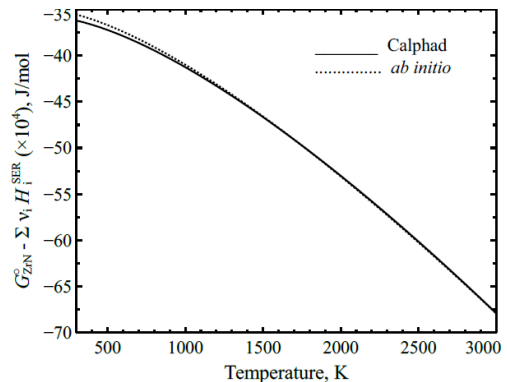


Figure 4. Comparison of calculated and *ab initio* Gibbs energy of ZrN

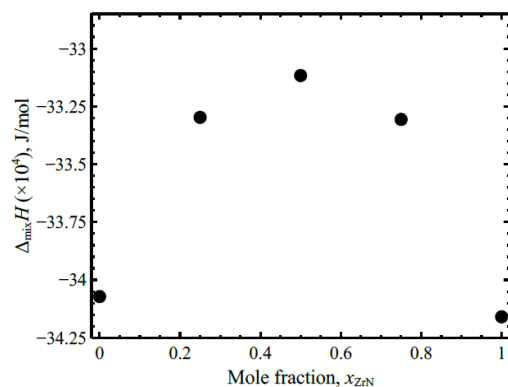


Figure 5. Enthalpy of mixing of TiN and ZrN computed using SQS

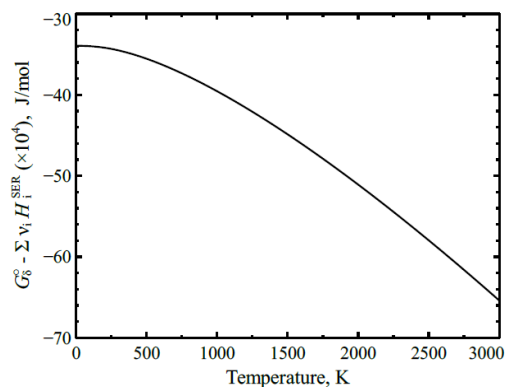


Figure 6. Gibbs energy of δ -phase of composition corresponding to Zr_{0.25}Ti_{0.75}N calculated using PHONON

(Figure 5). The Gibbs energy of formation of one of the compositions of the mixed nitride (δ -phase) corresponding to the formula $Zr_{0.25}Ti_{0.75}N$ was calculated using harmonic approximation is shown in Figure 6. The calculations for other SQS structures failed due to negative phonon frequencies.

In order to model the Gibbs energy functions of the Ti-Zr-N system, the thermodynamic descriptions for Zr-N from present work as well as Ti-N and Ti-Zr from [29] and [30], respectively, were combined. The model parameters for the δ phase were optimized with the *ab initio* thermochemical data as input. Figure 7 shows the calculated TiN-ZrN section. The predicted critical temperature and composition of the miscibility gap are 1844 K and 0.34 (x_{ZrN}), respectively. The partial isothermal section at 1473 K indicates the presence of δ -phase miscibility gap, as shown in Figure 8.

4.4. Si-Zr-N system

Experimental data indicate that the dissolution of nitrogen makes Zr_5Si_3 phase stable down to room temperature in Si-Zr-N system. The phase equilibria at 1273 and 1573 K were presented in the form of isothermal sections in the review by [31]. *Ab initio* calculations were performed for Zr_5Si_3N end-member since there are no experimental thermochemical data available for this system. The calculations predict it $\Delta_f H_{298}^0$ to be -968142 J/mol. The C_p° as a function of temperature, obtained using QHA is shown in Figure 9. The $C_p^\circ(T)$ values were fitted to relevant expressions and the Gibbs energy functions similar to Equation 15 were obtained by integration. A preliminary version of the Gibbs energy description for the ternary system is obtained by combining Gibbs energy functions of Si-N and Zr-N from the present work and the modified thermodynamic description of Si-Zr system from [32]. The Gibbs energy parameters for Zr_5Si_3N were optimized with the *ab initio* thermochemical data and the experimental constitutional data. The calculated isothermal sections at 1273 and 1573 K using the parameters obtained in this work and its comparison with experimental data from [31] are shown in Figures 10a and 10b, respectively.

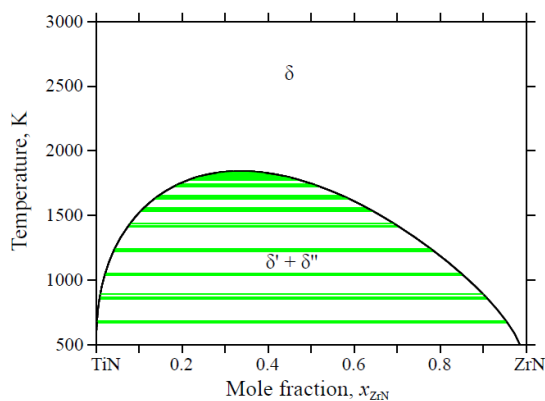


Figure 7. Calculated TiN-ZrN section

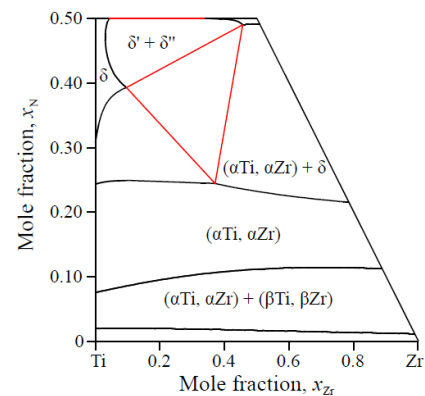


Figure 8. Calculated partial isothermal section at 1473 K

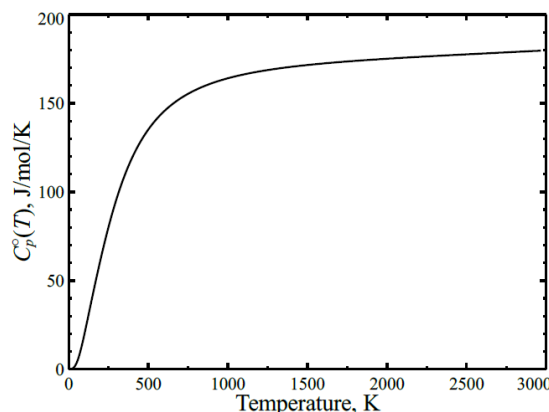


Figure 9. Calculated C_p° for Zr_5Si_3N using QHA

The change in the disposition of the tie-triangles between $\beta\text{Si}_3\text{N}_4$, ZrN, ZrSi, and ZrSi₂ at 1273 K and 1573 K indicates the presence of a U-type invariant reaction between these temperatures. The calculated U-type invariant reaction ($\text{Si}_3\text{N}_4 + \text{ZrSi} \rightleftharpoons \text{ZrSi}_2 + \text{ZrN}$) temperature is 1382 K. It is worth mentioning that when the Gibbs energy descriptions for the Si-N system from [24] was used, this reaction occurred at <500 K, which is inconsistent with the experimental data.

5. Conclusions

The present work was aimed at obtaining the thermodynamic descriptions for Si-Zr-N and Ti-Zr-N systems using the CALPHAD method. *Ab initio* calculations were used extensively to improve the quality of the Gibbs energy functions. Some of the key findings from this work are: $\beta\text{Si}_3\text{N}_4$ is thermodynamically more stable than $\alpha\text{Si}_3\text{N}_4$; the critical point of the miscibility gap in δ -phase was estimated to be 1844 K and 0.35 x_{ZrN} in Ti-Zr-N system; U-type invariant reaction temperature is calculated to be 1382 K in Si-Zr-N system.

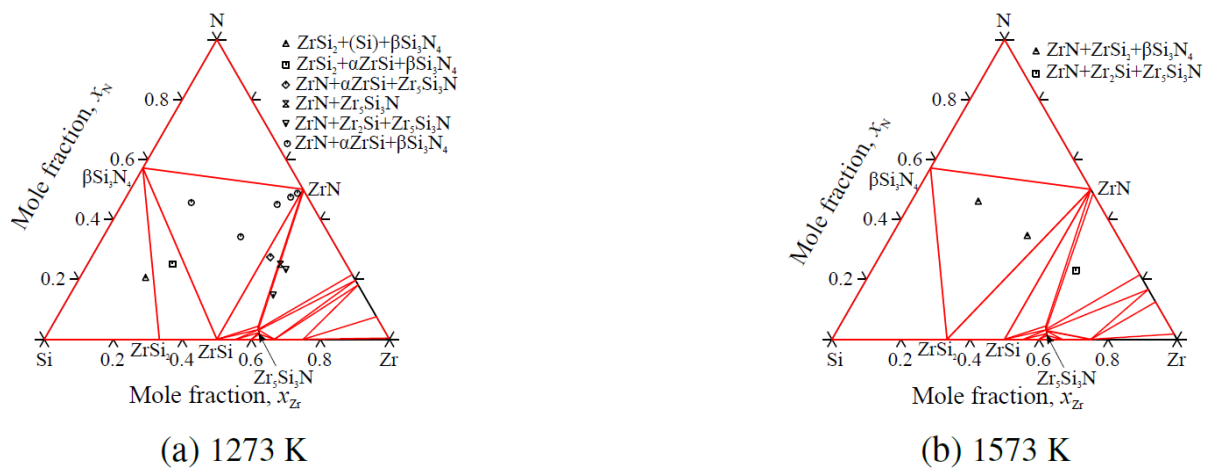


Figure 10. Comparison of calculated isothermal sections at 1273 K and 1573 K with experimental data from [31]

References

- [1] Musil J, Daniel R, Zeman P, Takai O, 'Structure and properties of magnetron sputtered Zr-Si-N films with a high (≤ 25 at.%) Si content', *Thin Solid Films*, 2005 478 238–247.
- [2] Nose M, Zhou M, Nagae T, Mae T, Yokota M, Saji S, 'Properties of Zr-Si-N coatings prepared by RF reactive sputtering', *Surf. Coat. Technol.*, 2000 132 163–168.
- [3] Knotek O, Böhmer M, Leyendecker T, Jungblut F, 'The structure and composition of Ti-Zr-N, Ti-Al-Zr-N and Ti-Al-V-N coatings', *Mater. Sci. Eng., A*, 1988 105 481–488.
- [4] Knotek O, Barimani A, 'On spinodal decomposition in magnetron-sputtered (Ti, Zr) nitride and carbide thin films', *Thin Solid Films*, 1989 174 51–56.
- [5] Sundman B, Jansson B, Andersson J O, 'The Thermo-Calc databank system', *Calphad*, 1985 9 153–190.
- [6] Van Laar J J, 'Melting or solidification curves in binary system', *Z Phys. Chem.*, 1908 63 216.
- [7] Kaufman L, Bernstein H, *Computer calculation of phase diagrams. With special reference to refractory metals*, Academic press, 1970.
- [8] Dinsdale A T, 'SGTE data for pure elements', *Calphad*, 1991 15 317–425.
- [9] Redlich O, Kister A T, 'Algebraic representation of thermodynamic properties and the classification of solutions', *Ind. Eng. Chem.*, 1948 40 345–348.
- [10] Muggianu Y M, Bambino M, Bros J P, 'Enthalpy of Formation of Liquid Bi-Sn-Ga Alloys at 723 K, Choice of an Analytical Expression of Integral and Partial Excess Quantities of Mixing', *J. Chim.Phys.*, 1973 72 83–88.
- [11] Temkin M, 'Mixtures of fused salts as ionic solutions', *Acta Phys. Chem., USSR*, 1945 20 411.
- [12] Hillert M, Staffansson L I, 'Regular-solution model for stoichiometric phases and ionic melts', *Acta Chem. Scand.*, 1970 24 3618–3626.
- [13] Harvig H, 'Extended version of the regular solution model for stoichiometric phases and ionic melts', *Acta Chem. Scand.*, 1971 25 3199–3204.
- [14] Sundman B, Ågren J, 'A regular solution model for phases with several components and sublattices, suitable for computer applications', *J. Phys. Chem. Solids.*, 1981 42 297–301.
- [15] Miedema A R, 'The electronegativity parameter for transition metals: heat of formation and charge transfer in alloys', *J. Less-Common Met.*, 1973 32 117–136.
- [16] Kresse G, Furthmüller J, 'Efficiency of ab-initio total energy calculations for metals and semiconductors using a plane-wave basis set', *Comput. Mater. Sci.*, 1996 6 15–50.
- [17] Monkhorst H J, Pack J D, 'Special points for Brillouin-zone integrations', *Phys. Rev. B*, 1976 13 5188.
- [18] Blöchl P E, Jepsen O, Andersen O K, 'Improved tetrahedron method for Brillouin-zone integrations', *Phys. Rev. B*, 1994 49 16223.
- [19] Van de Walle A, Tiwary P, De Jong M, Olmsted D, Asta M, Dick A, Shin D, Wang Y, Chen L Q, Liu Z K, 'Efficient stochastic generation of special quasirandom structures', *Calphad*, 2013 42 13–18.
- [20] Van de Walle A, Asta M, Ceder G, 'The alloy theoretic automated toolkit: A user guide', *Calphad*, 2002 26 539–553.
- [21] Parlinski K, Li Z, Kawazoe Y, 'First-principles determination of the soft mode in cubic ZrO_2 ', *Phys. Rev. Lett.*, 1997 78 4063.
- [22] Togo A, Tanaka I, 'First principles phonon calculations in materials science', *Scr. Mater.*, 2015 108 1–5.
- [23] Jansson B, 'Ph.D. thesis', Division of Physical Metallurgy, Royal Institute of Technology, Stockholm, Sweden., 1984 .
- [24] Ma X, Li C, Wang F, Zhang W, 'Thermodynamic assessment of the Si-N system', *Calphad*, 2003 27(4) 383–388.
- [25] Ma X, Li C, Bai K, Wu P, Zhang W, 'Thermodynamic assessment of the Zr-N system', *J. Alloys Compd.*, 2004 373 194–201.
- [26] Qiu C, Opalka S M, Olson G B, Anton D L, 'The Na-H system: from first-principles calculations to thermodynamic modeling', *Int. J. Mat. Res.*, 2006 97 845–853.
- [27] Domagala R F, McPherson D J, Hansen M, 'System zirconium-nitrogen', *Trans. AIME.*, 1956 8 98–105.

- [28] Yang G Y, Etchessahar E, Bars J P, Portier R, Debuigne J, ‘A miscibility gap in the FCC δ -nitride region of the ternary system Titanium-Zirconium-Nitrogen’ , *Scr. Metall. Mater.*, 1994 31 903–908.
- [29] Jonsson S, ‘Assessment of the Ti-N system’ , *Z. Metallkd.*, 1996 87 691–702.
- [30] Sridar S, Kumar R, Hari Kumar K C, ‘Thermodynamic modelling of Ti-Zr-N system’ , *Calphad*, 2017 56 102–107.
- [31] Rogl P, Schuster J C, Boron Nitride and Silicon Nitride Systems, Technical report, DTIC Document, 1991.
- [32] Chen H, Zheng F, Liu H, Liu L, Jin Z, ‘Thermodynamic assessment of B–Zr and Si–Zr binary systems’ , *J. Alloys Compd.*, 2009 468 209–216.